Proceedings of the ASME 2015 Pressure Vessels and Piping Conference
PVP2015
July 19-23, 2015, Boston, Massachusetts, USA

PVP2015-45325

CASS FRACTURE TESTS USING FLAT PLATE SPECIMENS WITH A SURFACE FLAW

Kiminobu Hojo
Mitsubishi Heavy Industries, Ltd.
Nuclear Component Designing Department
Nuclear Energy Systems Div.
1-1, Wadasaki-cho 1-chome,
Hyogo-ku, Kobe, 652-8585
Japan

Wataru Nishi
Mitsubishi Heavy Industries, Ltd.
Nuclear Component Designing Department
Nuclear Energy Systems Div.
1-1, Wadasaki-cho 1-chome,
Hyogo-ku, Kobe, 652-8585
Japan

Shotaro Hayashi
Mitsubishi Heavy Industries, Ltd.
Structure Laboratory
Takasago R&D Center
2-1-1, Shinhama Arai-cho
Takasago, 676-8686 Japan

ABSTRACT

JSME rules for fitness for service have flaw acceptance rules for cast austenitic stainless steel (CASS) pipes. They allow applying two-parameter and elastic-plastic fracture mechanics methods using Z-factor. However they do not clearly describe whether limit load method is applicable for the case of no or low thermal aging condition. The authors performed tensile fracture tests using flat plate specimens with a surface flaw and confirmed that limit load method is applicable in the conditions of no thermal aging and even fully saturated thermal aging with high ferrite number. Also the plate with a shallow flaw ruptured at the critical stress defined by nominal stress at rupture-flaw depth curve in the code case which was determined by the similar flat plate tests of stainless steel or nickel alloy specimens. These results will be reflected to the revision of the code.

NOMENCLATURE

σ_y	yield strength or 0.2% proof stress
σ_B	tensile strength
σ_f	flow stress
σ_c	critical fracture stress
Δa	crack growth amount
COD	crack opening displacement
E	Young's modulus
h	thickness
J_Q	J at ductile crack initiation in accordance with ASTM E813-89
J_6	J at Δa=6mm
$P(t,T)$	aging parameter
EPC	electric potential change
FAC	failure assessment curve of two parameter method
SC	screening criteria of two parameter method

INTRODUCTION

Primary coolant piping of operating PWR plants is made of CASS, which has good resistance to corrosion or SCC. On the other hand CASS is susceptible to thermal aging and has low detectability of flaws because of its special micro structure. Due to decreasing ductility by thermal aging, fracture mode of CASS changes from plastic collapse to ductile fracture. Tensile property and fracture toughness of CASS are affected by time and temperature of thermal aging. Kawaguchi et al. [1-3] and Chopra [4-9] proposed thermal aging prediction model for material properties of this material.

JSME rules for fitness for service have flaw acceptance rules for CASS piping. They allow using two-parameter method and elastic-plastic fracture mechanics method by Z-factor. Two-parameter method is capable to evaluate fracture mode from plastic collapse to brittle fracture by a parameter for material mechanics 'stress' and a parameter for fracture mechanics 'stress intensity factor'. However they do not clearly describe whether limit load method is applicable for the case of no or low thermal aging condition. Also neither of JSME rules, ASME Section XI, nor RSE-M incorporates any prediction models of thermal aging. For precise flaw evaluation the degradation model should be described in the codes.

In these circumstances the authors performed tensile fracture tests using flat plate specimens with a surface flaw and

confirmed the fracture mode of the specimens which were exposed in thermal aging or unaging condition to confirm a suitable fracture evaluation method. From the experimental results the applicability of the flaw acceptance rules in the existing code was verified for CASS material.

FRACTURE TEST

TEST CONDITION

Table 1 shows the fracture tests of the flat plates. Seven specimens were produced. The ferrite numbers were calculated in accordance with ASTM A800/A800M-91 and they were nearly 10% and 20%. Specimens A1-A6 were made of base metal of JIS G 5121 SCS14 (corresponding to CF8M). Specimen A7 has a welding joint parallel to tensile direction to simulate an axial flaw on a weld joint of a pipe. The specimens of base metal have semi-elliptical flaws with a parameter of depth 0.1*t* to 0.7*t* to confirm dependency of flaw depth on fracture stress. The target flaw length of each specimen was 38mm, but actual lengths were 29-39 mm. Before the fracture tests all specimens except A5 were exposed in thermal aging condition 465°C-5000h which is close to fully saturated condition. The aging temperature was relatively higher than that of Kawaguchi [3], but it was chosen by the time frame of the research. The effect on the thermal degradation mode was predicted small due to short aging time.

TABLE 1 FRACTURE TESTS MATRIX

Specimen#	Ferrite #	Material	Flaw depth *a/h*	Aspect ratio *a/l*	Aged/ Unaged
A1	9.3	Base	0.1	0.06	Aged
A2	9.3	Base	0.2	0.1	Aged
A3	9.7	Base	0.5	0.3	Aged
A4	9.7	Base	0.7	0.6	Aged
A5	10.5	Base	0.3	0.2	Unaged
A6	18.9	Base	0.5	0.3	Aged
A7	18.9	Weld	0.5	0.3	Aged

TEST SPECIMEN

Geometry of the fracture test specimen is shown in Fig. 1. Thickness of the specimen was 25mm which is equal to that of 1TCT specimen. The width was 100mm which should have little effect on fracture stress comparing with a wider specimen by a pre-FE analysis. Also the pre-analysis showed that the fracture mode and fracture stress of the plate specimen were almost same as those of a cylindrical specimen of the equivalent thickness of primary coolant pipe with an axial flaw whose detectable size has less margin to fracture than a circumferential flaw. At the center of the specimen an EDM notch was introduced and afterward a fatigue crack was added by cyclic tensile or bending load.

The weld joint specimen A7 was produced by SMAW simulating the actual welding condition. A7 specimen was tested for confirmation of residual stress effect on fracture load.

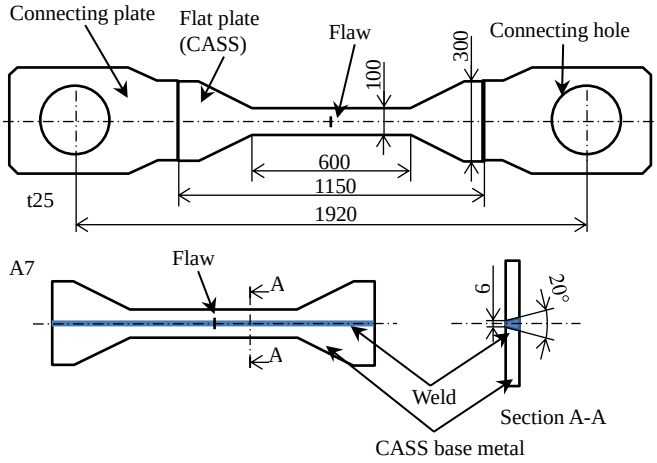

FIG. 1 FLAT PLATE SPECIMEN FOR FRACTURE TEST

TEST APPARATUS

Figure 2 shows the test apparatus and test specimen for the flat plate fracture test. One end of the specimen was fixed at the frame and the other end was connected to the tension bar. The loading capacity was 4000 kN and the maximum stroke was 200 mm. The test temperature was 325°C by heater and insulating material. The center of the specimen was visible to observe the crack opening behavior by adjusting the location of insulating material based on heat conduction analysis. The measured items were applied load, strain, *COD*, distance between the pins, EPC for change of flaw depth, temperature of the specimen, and video for observation of vicinity of a flaw.

FIG. 2 TEST APPARATUS AND TEST SPECIMEN

TEST RESULT

A summary of the fracture tests are shown in Table 2. Figure 3 shows examples of load-COD curves. EPC curves also are seen in the figure. *F*i is the estimated initiation point of ductile crack extension by EPC. Specimen A3 and A6 had similar size of flaws. The difference of maximum loads between both specimens is nearly the same within 2%. Similarly A2 and A5 have within nearly same size of flaws, and the difference of the maximum loads is 2%. On the other hand the difference of the maximum *COD* for each case is quite large, two times or more. Large ferrite number or aging gave large effect on ductility of CASS, not on the maximum load or stress of structure. The remarkable point is that there is no difference between the maximum stress of the low ferrite material specimen A3 and high ferrite material specimen A6 with similar size flaws. Thermal aging affects the fracture mode, but does not the maximum load or stress.

TABLE 2 SUMMARY OF FLAT PLATE TESTS

Specimen	Ferrite	Conditions			Max load (kN)	Max *COD* (mm)
		Mat.	Aged/ Unaged	*a/h*		
A1	Low (10%)	Base	Aged	0.1	1035	4.7
A2				0.2	879	5.3
A3				0.5	771	6.9
A4				0.7	712	6.5
A5			Unaged	0.3	897	10.4
A6	High (19%)	Base	Aged	0.5	787	2.4
A7		Weld		0.5	779	2.0

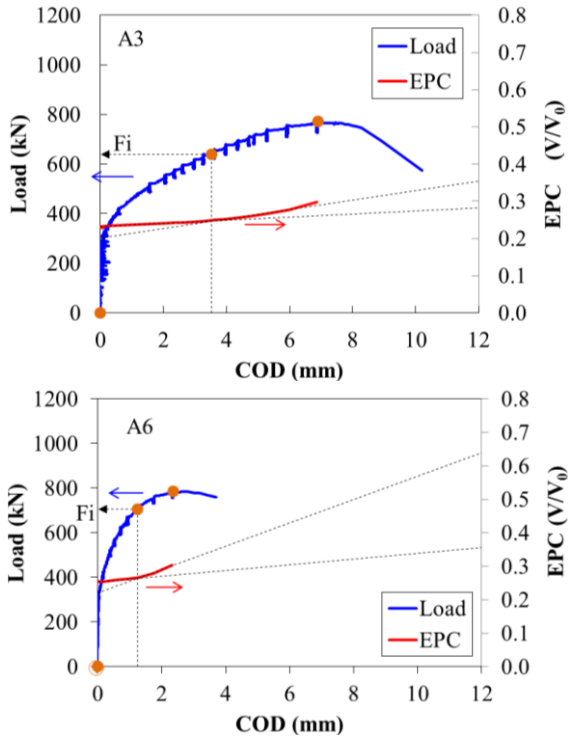

FIG. 3 LOAD AND EPC-COD CURVE

Welding effect is negligible from the results of A6 and A7.

On the fracture surface of all specimens dimple were observed.

MATERIAL TEST

For evaluation of the fracture test of the flat plate specimens, tensile and fracture toughness tests were conducted.

TEST CONDITON

Material of the specimens was the same as the flat plate specimens, SCS14A (CF8M). Aged material was exposed in the same condition of the flat plate specimens, 465°C-5000h.

The test matrix of tensile tests is shown in Table 3. The specimens were produced in accordance with JIS14A, the diameter of 10mm, and the gauge length of 50mm. The tests were conducted by JIS G 0567 (2012), and the test temperature was 325°C in air.

TABLE 3 TEST MATRIX OF TENSILE TESTS

Specimen #	Production method	Ferrite #	Material	Aged/ Unaged
B1	Static casting	Low (10%)	Base	Aged
B2				Unaged
B3			Weld	Aged
B4		High (19%)	Base	Aged
B5			Weld	Aged
B6-0	Centrifugal casting	Low(10%)	Base	Unaged
B6				Aged
B7-0		High(19%)	Base	Unaged
B7				Aged

The matrix of fracture toughness tests is shown in Table 4. The aging condition and test temperature of the fracture toughness tests were the same as the tensile tests. As the specimens were extracted from the flat plate, 1/2TCT specimens were used. The tests were performed in accordance with ASTM E813-89E01 [10] for comparison with Kawaguchi's data[1].

TABLE 4 TEST MATRIX OF FRACTURE TESTS

Specimen #	Production method	Ferrite #	Material	Aged/ Unaged
C1	Static casting	Low (10%)	Base	Aged
C2				Unaged
C3			Weld	Aged
C4		High (19%)	Base	Aged
C5			Weld	Aged
C6-0	Centrifugal casting	Low(10%)	Base	Unaged
C6				Aged
C7-0		High(19%)	Base	Unaged
C7				Aged

TEST RESULT

Tensile test

The result of the tensile tests is shown in Table 5. Figure 4 and Figure 5 show the ratio of ultimate strength after aging to unaged one vs. $P(t, T)$ [3] relations in the case of low and high ferrite numbers. $P(t, T)$ can be expressed by Equation (1).

$$P(t,T) = \log(t) + 0.4343\frac{Q}{R}\exp\left(\frac{1}{673.2} - \frac{1}{T}\right) \quad (1)$$

Here t is aging time, T is temperature, Q is activation energy (100kJ/mol) and R is gas constant.

In the figures the data of the material codes A to E are referred from the data of A-A to A-E of Kawaguchi [3]. For the centrifugal cast material the ratios of the present tests are nearly equal to or a little smaller than those of Kawaguchi. The reason of lower ratios of the present data seems scatter. Static casting material has lower strength than centrifugal casting.

TABLE 5 TEST MATRIX AND RESULT OF TENSILE TESTS

Case #	Production method	Ferrite #	Mat.	Aged/ Unaged	σ_y (MPa)	σ_B (MPa)	σ_f (MPa)
B1	Static casting	9.3	Base	Aged	143	416	280
					153	443	298
B2		10.5		Unaged	155	407	281
					155	405	280
B3		9.3	Weld	Aged	353	500	427
					352	496	424
B4		18.9	Base	Aged	182	553	368
					198	541	370
B5		18.9	Weld	Aged	347	502	425
					350	498	424
B6-0	Centrifugal casting	10.2	Base	Unaged	143	401	272
					143	405	274
B6				Aged	140	471	306
					136	463	300
B7-0		20.3		Unaged	181	480	331
					187	485	336
B7				Aged	178	549	364
					181	549	365

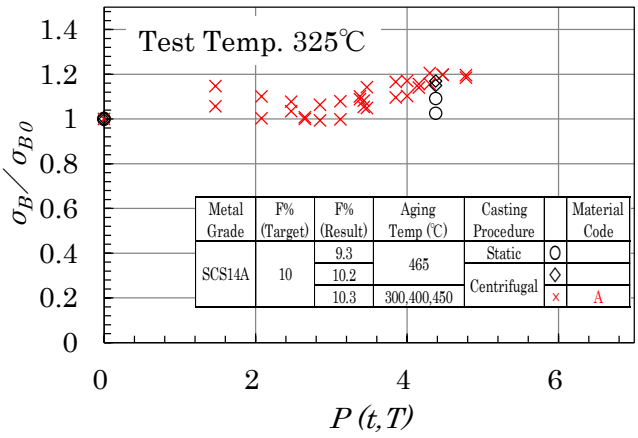

FIG. 4 RATIO OF σ_B AFTER AGING TO UNAGED σ_{B0} AGING PARAMETER RELATION (LOW FERRITE NUMBER)

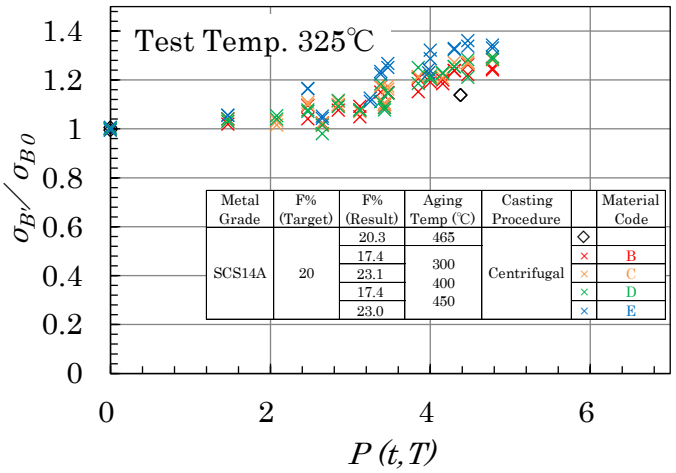

FIG. 5 RATIO OF σ_B AFTER AGING TO UNAGED σ_{B0} AGING PARAMETER RELATION (HIGH FERRITE NUMBER)

Fracture toughness test

Table 6 shows the result of the fracture toughness tests. Figure 6 and Figure 7 show examples of J-R curve of aged and unaged material with low and high ferrite numbers. These curves were used for fracture evaluation of the flat plate fracture tests. The invalid data of most of the test results means that the material still is kept ductile even after long thermal aging with high ferrite number.

TABLE 6 TEST MATRIX AND RESULT OF FRACTURE TESTS

Case #	Production method	Ferrite #	Mat.	Aged/ Unaged	J_Q (kJ/m^2)	J_6 (kJ/m^2)	valid/ invalid
C1	Static casting	9.3	Base	Aged	249	1331	invalid
					243	1104	invalid
C2		10.5		Unaged	509	1345	invalid
					725	1463	invalid
C3		9.3	Weld	Aged	115	458	invalid
					100	589	invalid
C4		18.9	Base	Aged	193	387	invalid
					159	382	invalid
C5		18.9	Weld	Aged	110	428	invalid
					113	443	valid
C6-0	Centrifugal casting	10.2	Base	Unaged	2380	2818	invalid
					2547	2786	invalid
C6				Aged	463	1321	invalid
					397	1318	invalid
C7-0		20.3		Unaged	1242	2071	invalid
					1412	2369	invalid
C7				Aged	255	803	invalid
					195	876	invalid

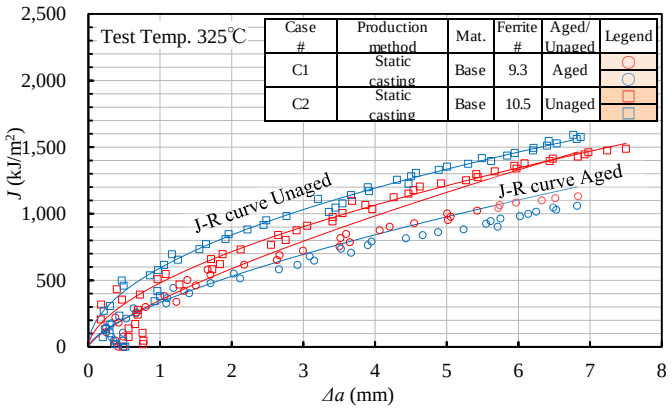

FIG. 6 J-R CURVE OF LOW FERRITE NUMBER MATERIAL

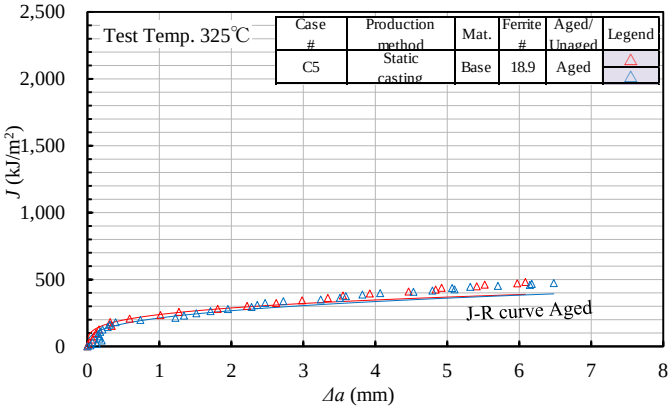

FIG. 7 J-R CURVE OF HIGH FERRITE NUMBER MATERIAL

ANALYSIS

ANALYSIS CONDITION

In order to simulate the fracture tests of the flat plate specimens, limit load method and two-parameter methods of JSME rules for fitness for service were applied.

FE model

To calculate J-integral FE analysis was performed using Abaqus Ver.6.8. An example of the FE model (SPECIMEN A3) is shown in Figure 8. A quarter of the test specimen was modeled. The element type was 8 node brick element and the numbers of nodes and elements were 33,730 and 29,950 respectively.

The true stress-strain curve and J-R curve for the FE analysis were used from the data obtained by MATERIAL TEST chapter.

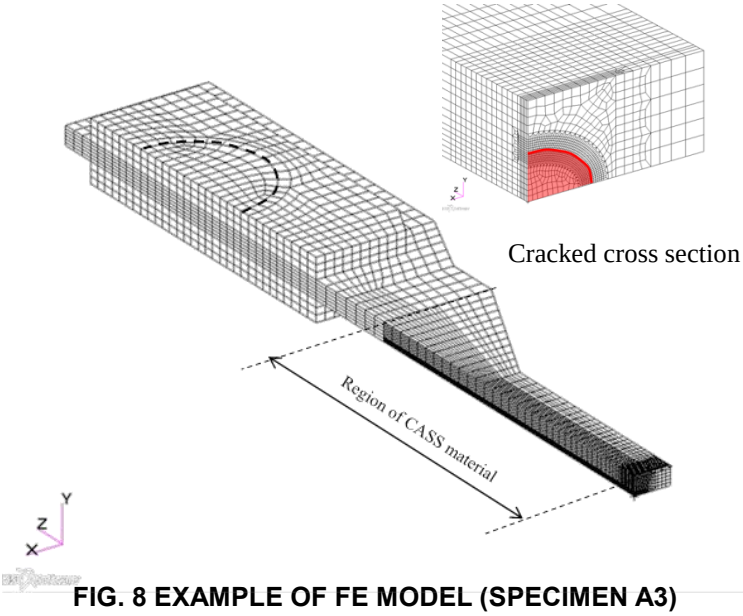

FIG. 8 EXAMPLE OF FE MODEL (SPECIMEN A3)

Evaluation method

The equation of limit load was based on Dillstrom[11]. For the critical material stress in the equation, flow stress σ_f was used. The code case of JSME rules for fitness for service has introduced the critical fracture stress σ_c dependent on the crack depth for the case of shallow crack whose depth is less than 50% of thickness. σ_c was also applied for the limit load evaluation.

For Two-parameter method the same equation of limit load as Ref. [10] was used for S_r of FAC. J-integral for K_r of FAC was calculated by FE analysis. J_e was converted from K which was obtained from JSME rules for fitness for service. The cutoff of FAC was set as σ_f/σ_y. During the ductile crack growth for ductile instability analysis the aspect ratio a/l was kept constant.

ANALYSIS RESULT

Figure 9 is an example of the comparison between the measured load-*COD* curve and that from FE analysis in the case of SPECIMEN A3. The FE result agrees well with the experiment, but and it is slightly larger. The reason is estimated that small blocks were attached near the crack to measure *COD* and the additional moment arm of the blocks from the specimen's surface had got to be neglected on the measured *COD* when the plastic deformation on the cracked cross section of the test specimen evolved. In the experiment the maximum load was measured because the plastic collapse and the specimen break occurred. On the other hand the FE model kept the initial crack shape during increasing the load, and that caused increasing the load-*COD* curve monotonically.

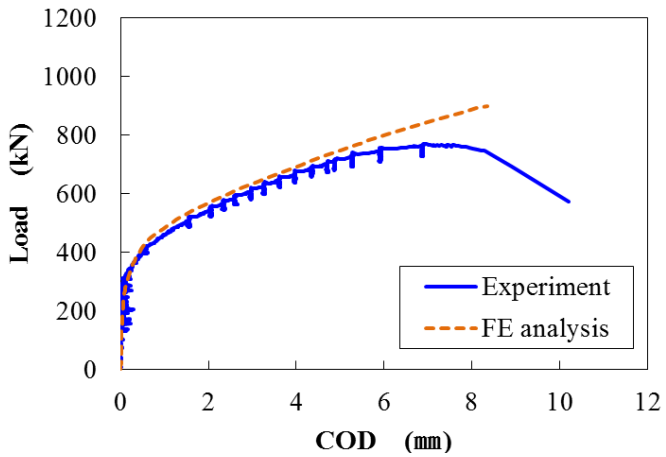

FIG. 9 LOAD-COD CURVE (SPECIMEN A3)

Figure 10 shows the summary of the comparison between the experimental maximum stress and the predicted ones due to limit load method due to the critical stress σ_f and σ_c, and two-parameter method due to the S_r cutoff σ_f/σ_y for the specimens A1-A6. The maximum stress was derived by the maximum load divided by the nominal cross section area.

From the figure, the followings observations are made. For the specimens of unaged and aged low ferrite material (A5 and A1-A4), limit load method and two-parameter method due to σ_f can conservatively predict the maximum load and basically both methods are equivalent. Limit load method due to σ_c can predict more precisely, and result shows that the σ_c criterion of the code case can be applicable to CASS in the condition of unaged material or aged material with low ferrite number. In these specimens the fracture mode was plastic collapse.

In the case of SPECIMEN A6 with high ferrite number limit load method was unconservative and two-parameter method is more suitable. This means the fracture mode shifted from plastic collapse to ductile fracture.

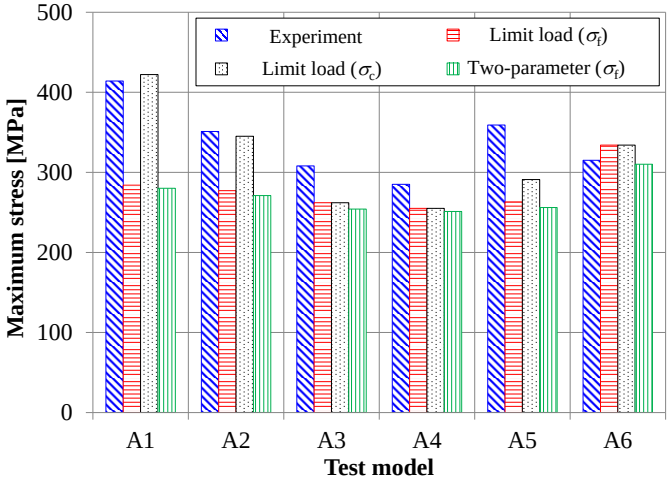

FIG. 10 COMPARISON OF THE MAXIMUM LOADS BETWEEN EXPERIMENT AND PREDICTION

EVALUATION

WELD JOINT

SPECIMEN A7 with high ferrite number included the weld joint vertical to the flaw was to simulate the axial flaw in a circumferential weld joint of a pipe. Both of the material data of the weld and base metal were used for prediction. Figure 11 shows the maximum stress of the experiment and predictions. The strength of the weld material is larger than that of the base metal. As a result the prediction of limit load method was unconservative than the case using the base metal because the area of the weld metal in the cracked cross section was smaller than that of the base metal. Two-parameter method can predict the maximum load of the experiment precisely for the both material conditions. Also the residual stress effect can be neglected in the evaluation.

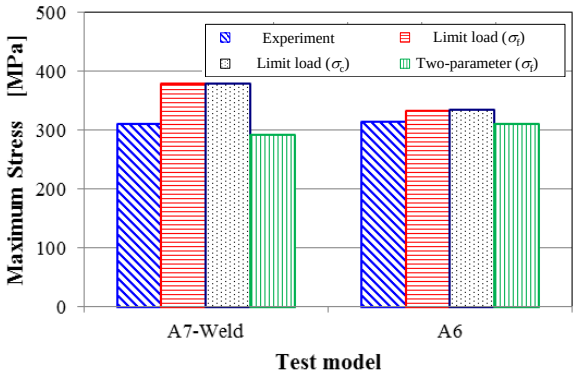

FIG. 11 COMPRISON OF THE MAXIMUM LOADS BETWEEN EXPERIMENT AND PREDICTION (SPECIMEN A7)

SCREANING CRITEREA

JSME rules for fitness for service introduced the screening criteria (SC) for selection of fracture evaluation method of ferritic piping because of various material strength and fracture toughness. This is similar to the case of CASS and applicability of SC of ferritic steel to CASS was examined. Figure 12 shows SC-a/t relation of the flat plate fracture tests. The fracture mode of SPECIMEN A6 and A7 were rather ductile fracture than plastic collapse and the SC value of SPECIMEN A6 is 0.17. Because 0.2 of the SC value is a bound between EPFM and limit load method in the current JSME code, the revision of 0.2 might be needed.

CONCLUSION

The tensile fracture tests using flat plate specimens of unaged or nearly full aged CASS with a surface flaw were performed to verify the fracture mode and prediction accuracy of the method in JSME rules for fitness for service.

As a result the fracture mode and maximum load were predicted by limit load method in the case of unaged or aged CASS with of low ferrite number. The fracture mode of the specimens of aged and high ferrite number was shifted to ductile fracture and two-parameter method should be chosen

for prediction of maximum load. SC for ferritic pipe in the JSME rules to be applicable, but further evaluation for the case of a primary coolant pipe is needed.

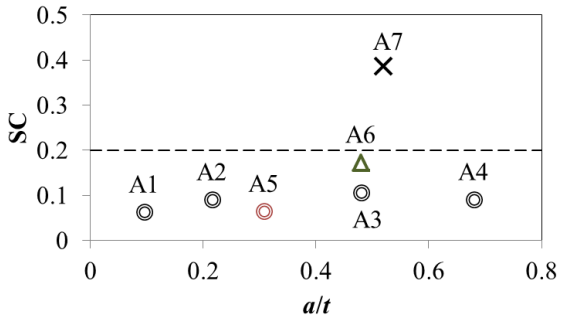

FIG. 12 SC OF FLAT PLATE SPECIMEN

ACKNOWLEDGMENTS

The research was funded by PWR owners group. The authors express acknowledgments to Kansai Electric Power Co., Hokkaido Electric Power Co., Shikoku Electric Power Co., Kyushu Electric Power Co., and Japan Atomic Power Co., especially Dr. Takehiko Sera. Also the authors thank Dr. Masayuki Kamaya and Dr. Naoki Ogawa, Ms. Mayumi Ochi, Mr. Fukuta and Mr. Takahisa Yamane for technical support and advice.

REFERENCES

[1] S. Kawaguchi, et al., The phase decomposition by thermal aging in duplex stainless steels, IIW DOC. IX-1747-94, September, 1994.
[2] S. Kawaguchi, et al., Microstructural Changes and Fracture Behavior of CF8M Duplex Stainless Steels after Long Term Aging, Nuclear Engineering and Design 174, 1997, p273-285.
[3] S. Kawaguchi, et al., Prediction Method of Tensile Properties and Fracture toughness of Thermally Aged Cast Duplex Stainless Steel Piping, PVP2005-71528, 2005 ASME Pressure Vessels and Piping Division Conference July 17-21, 2005.
[4] O. K. Chopra, et al., Effects of Low-Temperature Aging on the Mechanical Properties of Cast Stainless Steels, Proceedings on the Winter Annual Meetings of ASME, Boston, MA. December 13-18, 1987.
[5] O. K. Chopra, Long-term embrittlement of cast duplex stainless steels in LWR Systems, NUREG/CR-4744 Vol. 6, No.1, ANL-91/22, R5, August 1992.
[6] O. K. Chopra, et al., Evaluation of aging degradation of structural components, in Proceedings of the Aging Research Information Conference, NUREG/CP-0122, Vol. 2 1992, pp396-386.
[7] O. K. Chopra, et al., Assessment of Thermal Embrittlement of Cast Stainless Steels, NUREG/CR-6177 ANL-94/2, May 1994.
[8] O. K. Chopra, Thermal Aging of Cast Stainless Steels in LWR Systems: Estimation of mechanical properties, ASME PVP 1992.
[9] O. K. Chopra, Estimation of Fracture Toughness of Cast Stainless Steels During Thermal Aging in LWR Systems, NUREG/CR-4513, Rev. 1 ANL-93/22, 1994.

[10] ASTM E813-89E01, Test Method for J_{Ic}, A Measure of Fracture Toughness (Withdrawn 1997), ASTM International, West Conshohocken, PA, 1989.
[11] P. Dillstrom, and I. Sattari-Far, Limit Load Solutions for Surface Cracks in Plates and Cylinders, RSE R & D Report, No.2002/01, Det Norske Veritas AB, 2002.